FIRST LASING OF THE ALICE IR-FEL AT DARESBURY LABORATORY

D.J. Dunning, N.R. Thompson, J.A. Clarke, M. Surman, A.D. Smith, Y. Saveliev,
STFC Daresbury Laboratory and Cockcroft Institute, UK
S. Leonard, University of Manchester, UK

Abstract

We report the first lasing of an infra-red oscillator FEL installed at the test facility ALICE (Accelerators and Lasers In Combined Experiments) at the UK's Daresbury Laboratory. First lasing was achieved at a wavelength of 8μm in October 2010, making it the first FEL to successfully operate in the UK. This report describes the installed hardware, commissioning and first lasing, the first characterisation of the FEL performance and output, and further developments.

INTRODUCTION

An Infra-Red (IR) oscillator Free-Electron Laser (FEL) was recently installed into ALICE (**A**ccelerators and **L**asers **I**n **C**ombined **E**xperiments), the superconducting Energy Recovery Linac (ERL) accelerator test facility at Daresbury Laboratory in the United Kingdom. First lasing, at a wavelength of 8 μm, was observed in October 2010 with ALICE operating at an electron beam energy of 27.5 MeV. This is the first FEL to successfully operate in the UK. The FEL programme has been reported in previous publications, covering the design parameters [1, 2], expected output performance [3, 4] and first commissioning results [5]. Figure 1 shows the layout of the ALICE IR-FEL, and the nominal operating parameters are given in Table 1.

FEL COMPONENTS

Undulator

The undulator is a 40-period hybrid design, on loan from Jefferson Laboratory where it was previously used for the IR-DEMO FEL project. It has been converted for use on ALICE from fixed gap to variable gap to increase wavelength tuning range. At minimum operating gap of 12.1 mm the undulator parameter $K_{rms} \simeq 0.9$ giving a resonant wavelength of $\sim 8\mu$m at the normal ALICE electron beam energy of 27.5 MeV. The undulator vessel incorporates three beryllium wedges that are integral to the FEL alignment strategy. Each wedge has a 1 mm diameter hole which is used to define the reference FEL axis.

Optical Cavity

The cavity mirror vacuum vessels and motion systems are on loan from the CLIO FEL. Both upstream and downstream mechanisms provide pitch and yaw mirror motion, and the downstream mechanism also provides cavity length adjustment. The mirrors have diameter 38 mm and are copper with gold coating. Outcoupling is through an on-axis hole in the downstream mirror. The cavity geometry is symmetric and close to concentric. The cavity length is $L = 9.22438$ m such that the optical cavity round trip frequency matches the electron bunch repetition frequency of 16.25 MHz.

There are two permanently installed HeNe laser alignment systems - one for each of the optical cavity mirrors. The alignment systems operate by directing a HeNe beam along the reference axis of the cavity onto the mirror face. The reflected beam can be viewed on the central wedge, allowing the mirror angle to be measured. This system has proven to be effective (and repeatable) for the angular alignment of the cavity mirrors. The length of the optical cavity is measured indirectly using a laser tracker system and external targets on the cavity mirror vessels, with an estimated maximum error of 0.5 mm. The cavity length must therefore be scanned to establish the approximately $20\,\mu$m region for lasing.

Photon Diagnostics

To detect the spontaneous IR undulator radiation a Mercury Cadmium Telluride (MCT) detector operated at liquid nitrogen temperatures is installed beyond the downstream cavity mirror. The MCT signal is fed through a local pre-amplifier with variable gain before being transported out of the accelerator area to the control room. The pre-amplification is necessary to observe the low intensity spontaneous emission, and can be bypassed when lasing. A modulation of the MCT signal with a period of 61.5 ns, due to individual FEL pulses, is then observed indicating that the response time of the detector is fast enough to measure the cavity rise and decay to determine the FEL gain and cavity loss. The IR can also be diverted to a spectrometer based upon a Czerny Turner monochromator. This incorporates a second MCT detector for spectral measurements of the spontaneous emission and a less sensitive pyrodetector for the FEL emission.

Electron Beam

Electrons are produced using a high voltage DC photo electron gun, operating currently at 230 kV. For FEL operation the electron bunch repetition frequency is 16.25 MHz in macropulses of 100 μs (1625 bunches) which repeat at 10 Hz. After the gun the electrons are accelerated in a superconducting booster to 6.5 MeV. The RF phases of the two booster cavities are chosen such that the electron bunch exits with a small positive energy chirp (higher energy electrons at head of the bunch). This is to avoid lon-

Figure 1: Schematic of ALICE FEL systems (top) and panoramic photograph of the ALICE FEL (bottom).

gitudinal cross-over while the beam is not fully relativistic (space charge effects are still of importance) during transport to the SC linac, which then accelerates the electrons to 27.5 MeV.

The first arc, between the main linac and the four-dipole magnetic compression chicane upstream of the undulator, is a 180° triple-bend achromat, normally set for $R_{56} = 0$. The chicane has a static $R_{56} = 0.28$ m, requiring the linac to be set to an off-crest phase of $\sim 10°$ for optimal bunch compression. However, the compensation of the positive chirp from the booster requires the linac to be operated at $\sim 5°$ off-crest, resulting in a cumulative linac off-crest phase of $\sim 15°$. Quadrupoles in the arc can be used to modify the R_{56} slightly to optimise bunch compression in place of varying linac phase. The arc also has two sextupoles used to linearise, by varying T_{566}, the lowest-order curvature induced by the sinusoidal RF acceleration field.

The undulator arrays are vertical, giving horizontal focussing. The beam is therefore focussed to give a horizontal waist at the undulator entrance, with the waist radius set to $\sigma_x = (\varepsilon_n \lambda_w / 2\pi K_{rms})^{1/2}$ so that the beam divergence is matched to the horizontal focussing strength of the undulator. This gives constant beam radius which minimises the gain degradation due to betatron oscillations. In the vertical (y) plane there is no focussing, so the beam behaves as in a drift space. Here the gain is maximised with a waist in the undulator centre with the waist radius set to minimise the average beam radius over the undulator length.

COMMISSIONING OF THE FEL

Spontaneous emission from the undulator was first detected in February 2010. Measurements of the spectral width were then made to optimise the electron beam trajectory in the undulator—the narrowest linewidth and minimum peak wavelength correspond to the on-axis trajectory. Further details on these results are given in [5].

It was observed that the intensity of the spontaneous emission increased when the accelerator was set to give maximum compression (minimum bunch length), due to coherent enhancement of the undulator emission. The off-crest phase of the linac was varied to change the bunch compression. This correlated with the power variation of the coherently-enhanced broadband THz emission emitted from the final dipole in the bunch compression chicane. This has proved to be a useful diagnostic for confirmation of the correct longitudinal dynamics.

Phase coherence of the enhanced spontaneous emission was evident when scanning to find the correct cavity length for lasing. Periodic oscillations in the output intensity were observed as the cavity length was changed, with the period equal to half the emission wavelength. The explanation is that adjusting the cavity length by $\lambda_r/2$ changes the round trip length within the cavity by λ_r, so the oscillations are due to interference between emission from successive electron bunches. This demonstrates good pulse-to-pulse phase coherence and indicates that the temporal jitter Δt between successive electron bunches must be less than half an opti-

Table 1: ALICE IR-FEL Nominal Operating Parameters

Parameter	Notation	Value
ELECTRON BEAM		
Energy	E	27.5 MeV
Bunch Charge	Q	60-80 pC
FWHM Bunch Duration	Δt	$\simeq 1$ ps
Normalised Emittance	ε_n	10 mm-mrad
RMS Energy Spread	σ_E/E	0.5-0.7%
Repetition Frequency	f	16.25 MHz
Macropulse Duration		100 μs
Macropulse Frequency		10 Hz
UNDULATOR		
Type		Hybrid Planar
Period	λ_w	27 mm
Number of Periods	N	40
Minimum Gap	$g_{\min}$	12.1 mm
Undulator Parameter	$K_{\rm rms}$	0.9
OPTICAL CAVITY		
Type		Near-concentric
Cavity Length	L	9.2234 m
Mirror ROC	R	4.85 m
Rayleigh Length	Z_R	1.05 m
Mirror Material		Cu/Au
Outcoupling		Hole
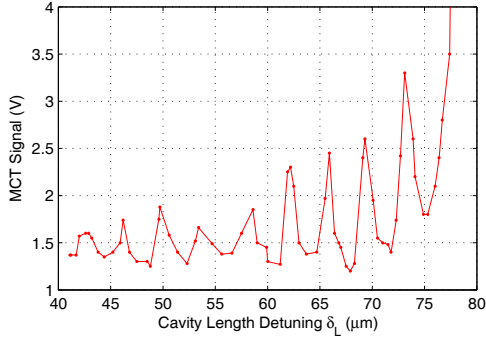
Figure 2: Variation of the spontaneous emission signal with cavity length detuning (relative to the encoder zero point).

cal period of the 8 μm emission, or $\Delta t \lesssim \lambda_r/2c = 13$ fs. The oscillations increase in intensity as the cavity length becomes closer to the correct length for lasing, so can be used to set the correct length. An example is shown in Fig. 2—clear oscillations in the spontaneous emission signal with a period of 4 μm were observed, becoming stronger towards the cavity length for lasing.

Several unsuccessful efforts to achieve lasing were made, indicating insufficient net gain. To reduce the cavity losses, the outcoupling mirror was replaced by one with a smaller hole, reducing from 1.5 mm radius to 0.75 mm. The operating bunch charge had been limited to 40 pC, at a repetition rate of 81.25 MHz, because the accelerating structures were unable to support a higher average current

while maintaining a constant electron beam energy along the macropulse. On 17th October 2010, a burst generator was installed as part of the photo-injector laser system to reduce the repetition rate by a factor of five to 16.25 MHz allowing the bunch charge to be increased to 80–100pC.

First Lasing

Lasing was first demonstrated on 23rd October 2010 at a wavelength of 8 μm, operating at a beam energy of 27.5 MeV and an electron bunch charge of 80 pC. The first measured cavity length detuning curve is shown in Fig. 3. This shows measured average power, normalised to the peak power observed, as a function of cavity length detuning δL from the synchronous cavity length $L = c/2f$ with $f = 16.25$ MHz. The width and shape of the detuning curve agree well with the simulations which were done in the one-dimensional oscillator FEL code FELO[6].
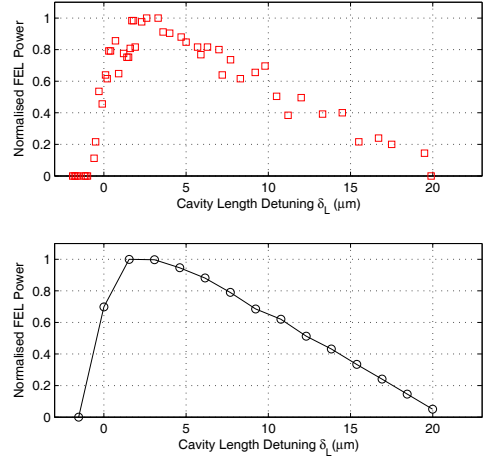

Figure 3: First measured FEL detuning curve (top) compared with simulation (bottom). The power is normalised to the peak of the curve, with the measured curve shifted on the x-axis to align with the simulation (since no precise measurement of the synchronous cavity length is made).

The FEL lased reliably during the next few days, before an ALICE shutdown commenced at the end of October. The maximum pulse energy observed over this period was 3.3 μJ in-vacuum immediately behind the outcoupling hole; this was determined indirectly from the measured average power, the known timing structure of the FEL output and the known transmission of the vacuum window between FEL and detectors. The conversion efficiency of electron beam power to FEL output power, given by $\eta_{FEL} = E_{PULSE}/QE$, with Q the bunch charge in Coulombs and E the electron beam energy in eV, was thus 0.15%. This is only 1/4 of the theoretical maximum efficiency (ignoring the hole outcoupling efficiency, estimated from simulations to be $\sim$50%), given by $\eta_{max} = 1/4N$ with N the number of undulator periods. The primary reason for this is that the outcoupling hole was set deliberately

small to reduce losses for the first attempts at lasing.

The FEL pulse length was estimated indirectly from the measured spectral width. The output pulses were assumed to be transform limited so that the time-bandwidth product is approximately one half, i.e. $\Delta\nu\Delta t = (1/\lambda)(\Delta\lambda/\lambda)\Delta z \simeq 0.5$, where Δ represents full-width half-maximum (FWHM) values. Therefore the FWHM pulse length is given by $\Delta t \simeq 0.5\lambda^2/(c\Delta\lambda)$. Peak power was calculated from pulse length and pulse energy. Figure 4 shows typical results, with various parameters plotted as a function of cavity length detuning. The pulse length is seen to vary from 0.8–1.5 ps over the cavity detuning range. The output parameters are summarised in Table 2.
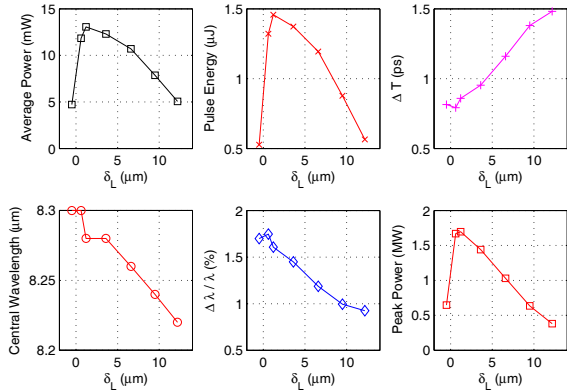
Figure 4: Average power, pulse energy, pulse length, central wavelength, bandwidth, and peak power plotted as a function of cavity length detuning δL.

The total cavity loss was determined to be $T = 0.06$ from MCT measurements of the cavity ringdown time. This matches the expected cavity loss factors which are 2% outcoupling, 2% due to diffraction from the hole within the cavity and 1% absorption in each FEL mirror. The small signal net gain N was determined from the observed exponential rise time, fitting the data only up to 10% of the saturation power. With the net gain and cavity loss determined, the small signal single pass gain $G = (N+T)/(1-T)$ was calculated. The maximum measured gain was $G = 22\%$ at a bunch charge of 70 pC. Using the observed electron beam parameters at this time, as given in Table 1, the predicted single pass gain is 24%, in good agreement. With an electron beam energy spread of 200 keV, the gain is reduced to approximately one third compared to a mono-energetic beam—work is ongoing to improve this.

Further Developments

The continuous tunability of the FEL wavelength has since been demonstrated. The undulator gap was varied between 12-16 mm and the lasing wavelength tuned from 8.0–5.75 μm. No alterations to the electron beam steering or focussing were required to maintain lasing over this range. Subsequently the steering was optimised and las-

Table 2: FEL Output Parameters, In-vacuum Immediately behind the Downstream Mirror

Parameter	Notation	Value
Wavelength	λ_r	5.0–8.0 μm
FWHM Bandwidth	$\Delta\lambda/\lambda$	0.9–1.8 %
Pulse Energy	E_{pulse}	$\leq$ 3.3 μJ
Peak Power	P_{peak}	$\leq$ 3.6 MW
Average Power	P_{avg}	$\leq$ 45 mW
Average Power (within macropulse)	$P_{\text{avg,pulse}}$	$\leq$ 53 W

ing was obtained at the shortest wavelength of 5 μm. Normalised FEL spectra are shown in Fig. 5. Higher harmonics of the FEL output have also been observed.
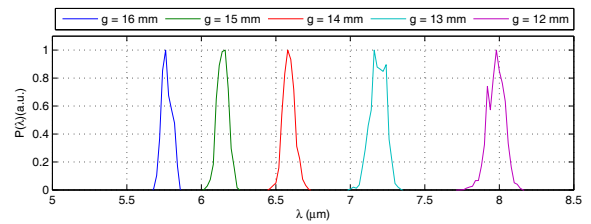

Figure 5: FEL Spectra for different undulator gaps.

The FEL output is now being transported to a dedicated diagnostics room for further characterisation. It is intended to reduce the optical cavity ROC to 4.75 m to enhance the FEL gain, and to use a larger outcoupling hole to optimise the FEL output. Upgrades are planned to the FEL diagnostics to enable single-macropulse FEL spectra and single-shot FEL pulse length measurements. A select programme of FEL physics and user experiments is planned.

ACKNOWLEDGEMENTS

REFERENCES

[1] N.R. Thompson, *ERL Prototype Free-Electron Laser*, internal report, erlp-ofel-rpt-0001, 2003.

[2] N.R. Thompson, *Design for an Infra-Red Oscillator FEL for the 4GLS Energy Recovery Linac Prototype* Proc. 25th Int. FEL Conf. (Tsukuba, Japan), II-15, 2003.

[3] D.J. Dunning et al. *3D Modelling of the ERLP IR-FEL* Proc. 29th Int. FEL Conf. (Novosibirsk, Russia), p167-170, 2007.

[4] D.J. Dunning et al. *Overview and Status of the ALICE IR-FEL* Proc. 31st Int. FEL Conf. (Liverpool, UK), p583-586, 2009.

[5] J.A. Clarke et al. *Status of the ALICE IR-FEL* Proc. 32nd Int. FEL Conf. (Malmo, Sweden), p41-44, 2010.

[6] B.W.J. McNeil et al. *FELO: A One-Dimensional Time-Dependent FEL Oscillator Code* Proc. 28th Int. FEL Conf. (Berlin, Germany), p59-62, 2006.